

Thrust and Electrical Power from Solid Propellant Microrockets

2. Actuators

William Lindsay, Dana Teasdale, Veljko Milanovic, Kristofer Pister, Carlos Fernandez-Pello
University of California, Berkeley

ABSTRACT

Progress has been made in the development of flying silicon. Fully self-contained MEMS rockets have been designed, fabricated and tested. A peak thrust of 4mN was obtained from a rocket with a mass of 0.98grams. This rocket was comprised of a 3.2mm inside diameter ceramic tube bonded to a silicon chip containing the rocket nozzle, igniter and an array of twelve thermopiles. One thermopile was measured during combustion and yielded 20microWatts of electrical power during a combustion event of approximately 10 seconds. Third-generation devices have demonstrated liftoff.

INTRODUCTION

Rocket design spans the spectrum of man-made lengthscales perhaps better than any other device ever created. In use today there are rockets measuring hundreds of meters in size, all the way down to one centimeter, and every size in between. Any child who has been in a hobby store knows that the best way to get a small mass as high as possible is with a rocket. It is therefore reasonable to assume that a microrocket might be the best means to imbue a silicon ship with mobility.

Mobile silicon is the goal of several research groups. Yeh et al are attempting to make silicon walk like a silicon-beetle [1]. Another bio-mimetic device is the Micro Flying Insect [2], which is like a silicon housefly. Microrockets have no biological model to mimic directly, but many plants and animals, even on the microscale, use accelerated flows to generate thrust [3].

The intended use for silicon Microrockets is as a deployment system for distributed sensor networks such as Smart-Dust [4]. An inexpensive device that could fly tens or hundreds of meters into the air, take a series of measurements and communicate with the home base, would be of great use to meteorologists, the military, etc.

In order to get large displacement one needs high energy density storage. Combustion is one way to cheaply obtain large quantities of energy from a small volume. Typical liquid hydrocarbon fuels have an energy density of around 40J/mm³ [6]. Commercial zinc-air batteries have an energy density of just over 5J/mm³ [7]. If this chemical energy can be efficiently converted to useful energy, a microscale combustion device could exceed the energy

density of batteries.

Many research projects are attempting to unleash the high energy density of fuels on the microscale. A micro gas turbine, a free-piston engine, and a rotary internal combustion engine are in development, among others [8], [9], [10]. These projects each face unfavorable scaling trends in efficiency. A large power plant can operate at 60% efficiency. A very large boat engine can approach 50%, while an automobile engine might reach 30%. A portable generator runs at 20%. The scaling of frictional and thermal losses can be blamed for this downward trend in efficiency with decreasing size, and 0% efficiency might happen well before 0 size. Solid-propellant rockets, as initially envisioned by Rossi [5], avoid some of these problems. First of all, thrust is a more direct product of combustion, requiring no complex energy conversion. The frictional losses inherent to moving parts are eliminated because there are no moving parts.

Liquid or gaseous fuels could also be used in microrockets, and would present a few major benefits. Liquid or gaseous fuels could flow for arbitrarily long times, and the devices could be refueled, whereas solid fuel microrockets are single-use devices. With a much simpler fabrication process, though, a solid-fuel rocket might be easier and cheaper to build than a liquid or gaseous fuel rocket would be to refuel.

In addition to thrust, combustion establishes thermal gradients in the structure of the rocket. These gradients can be spanned with thermopiles to generate useful electrical energy. High-efficiency Micro-thermopiles that are easily incorporated into the fabrication process have been reported in the literature [13].

ROCKET DYNAMICS BACKGROUND

The design of a millimeter scale rocket came out from an understanding of the scaling of the various forces to which every rocket is subjected. The simplified equation of motion is:

$$m(t)\ddot{x}(t) = F(t) - m(t)g \mp \frac{1}{2}C_D A\rho[\dot{x}(t)]^2 \quad (1)$$

This equation models the interrelationship of the thrust force, the body force due to gravity and the surface force

due to air-drag. The drag force is minus-or-plus because the direction of the drag force changes direction when the motion changes direction at the apex of the flight. Mass is a function of time because as propellant is consumed the remaining mass decreases. A drag coefficient (C_d) of unity can be assumed [11]. In exo-atmospheric flight, where the drag force is zero, the shape of the force vs. time curve has no effect on the final velocity. In endo-atmospheric flight, the magnitude of the thrust determines the terminal velocity of the rocket, and has a large effect on how fast, how far, and for how long the flight will proceed.

A piecewise-linear finite-difference model of equation (1) was constructed for several different force vs. time curves. Thrust forces varying from 1mN to 1kN were modeled. The duration of each force was chosen so the momentum for each thrust was 0.1N-sec, so the time for the 1mN force was 100sec, and the time for the 1kN force was 0.1ms, etc. To model fuel consumption, the rocket was considered to be a mass that decreased linearly from 250mg to 150mg during the thrust time. The above equations were modeled in a piecewise linear fashion for a rocket with a cross-sectional area of 25mm². The results of this model are shown in Figures 1, 2 and 3.

Figure 1 illustrates the maximum velocity as a function of the thrust force. The large force examples yielded similar velocities because the drag force was negligible in comparison to the thrust force so the full momentum under the thrust-time curve was "forced" onto the mass. The lower force examples reach terminal velocity before the thrust event reaches completion, and therefore become limited by the drag force. Supersonic drag has been ignored, overestimating the final velocity for the short duration high thrust examples, but as we see in Figure 2, this is unimportant.

The maximum altitude vs. thrust force is shown in Figure 2. The maximum altitude predicted in this analysis was 325 meters for a thrust force of 4mN acting for 25 seconds. The possibly counterintuitive conclusion is that high altitudes are achieved with a thrust force only slightly larger than the gravitational force. If the force is too large non-linear viscous drag dominates. If the force is too small, gravity dominates. The flight duration scales with maximum altitude, because the time it takes the mass to fall to the ground is the most time consuming event. Those predictions are plotted in Figure 3. The conclusion drawn from this analysis was that endo-atmospheric microrockets should be designed to produce moderate thrust for as long as possible.

COMBUSTION BACKGROUND AND SCALING

Getting the desired flight performance of a rocket depends in part on the choice of propellant. Propellants are rated by their specific impulse (I_{sp}), which has units of momentum per weight, which reduce to units of time. I_{sp} is defined as:

$$I_{sp} = \frac{\int F dt}{mg} \quad (2)$$

A higher I_{sp} indicates a more energetic propellant. Hydroxyl-Terminated Polybutadiene (HTPB) was selected as the fuel and Ammonium Perchlorate (AP) as the oxidizer.

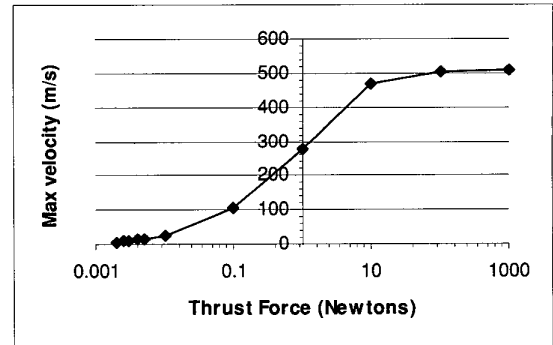


Figure 1: This plot shows the modeled maximum velocity achieved by a rocket as a function of thrust amplitude with total thrust held constant.

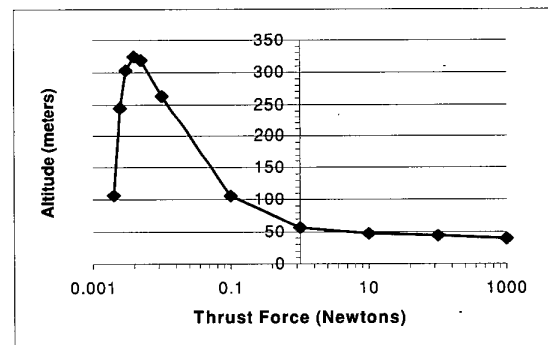


Figure 2: The maximum altitude. High max velocity from Figure 1 does not translate to high max altitude due to non-linear drag.

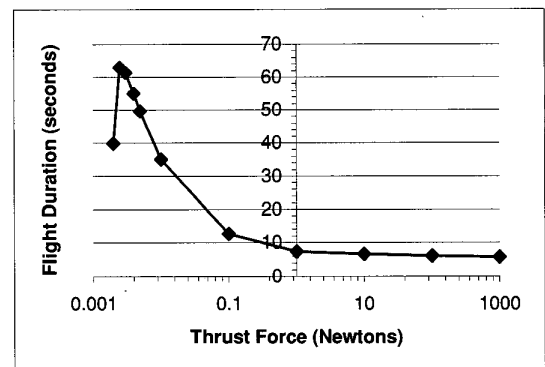


Figure 3: The simulations that reached the highest altitude also have the longest flight duration. The maximum predicted value was over one minute.

This propellant system (HTPB/AP) has a specific impulse of 256s under optimal conditions, or 2.5 times the value used in the simulations described above. The propellant is prepared by mixing fuel and oxidizer chemicals to form a paste that can be forced into a receptacle. The fuel is then cured at 130 degrees F for 24 hours, and it becomes solid, like hard rubber.

Rocket designers manipulate the thrust vs. time curve by controlling the surface area of the fuel grain. In a millimeter-scale rocket, the shape of the fuel grain will just take the shape of the combustion chamber, and that will influence the thrust curve. A prolonged thrust event can be achieved by choosing a propellant that burns slowly and/or by making the fuel grain long and thin.

Both these of these techniques bring up important considerations in thermal scaling. The heat generated in a reaction scales like its volume, but the heat conducted out of that volume scales like the surface area. Therefore if the surface area to volume ratio gets too large, thermal losses will quench the reaction and make combustion impossible. Long and thin combustion devices then severely limit the efficiency of the combustion. Choosing a slow burning fuel provides more time for heat to be conducted to the cold surfaces of the combustion chamber and might similarly limit efficiency. Very fast burning propellants, like gunpowder, can reduce thermal losses by burning very fast. This feature can be very useful in outer space, where there are no viscous drag forces. The MEMS digital propulsion system designed by TRW exploits this feature of explosive propellant [13], but we see from Figures 2 and 3 that explosive thrusts will not provide a suitable flight in air. The limitations of these thermal-scaling trends were explored in the first generation of microrocket.

DESIGN OF FIRST GENERATION ROCKET

Minimum performance specifications were chosen for the microrocket. Based on the best I_{sp} of HTPB/AP a goal of 100s was chosen. Fuel mass and burn time were set at 100mg and 5-10s, respectively. Based on the predictions developed above, the maximum altitude of 100m was the goal. The sensor system that comprises the payload was

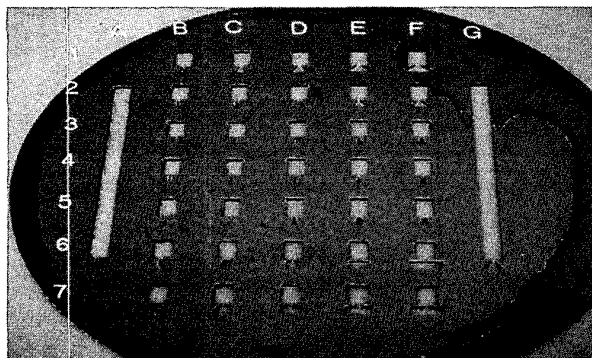


Figure 4: The first-generation rocket combustion chambers were made by etching through a silicon wafer.

expected to be one or more sensors, an optical communication system, computation, and power storage. This payload is expected to have a mass of approximately 1mg, and have power requirements of 10 μ W average and 10mW peak [4].

A silicon test wafer was processed to explore the thermal limits discussed above (see Figure 4). A batch of 37 rockets was etched by Deep Reactive Ion Etching (DRIE). Each hole was filled with propellant by smearing it in with a spatula; the volume was enclosed by gluing a glass slide to each side of the wafer. Similar devices were cut in 500micron thick samples of various other materials by traditional machining methods. Ignition could only be achieved with alumina ceramic as the chamber material.

Exploiting the favorable thermal properties of alumina ceramic, a two-piece rocket was developed. A ceramic cylinder with an inside diameter of 3.2mm was used as the combustion chamber. A MEMS die included the nozzle, igniter, and thermopiles for electrical power generation (see Figure 5). The nozzle was 1mm in

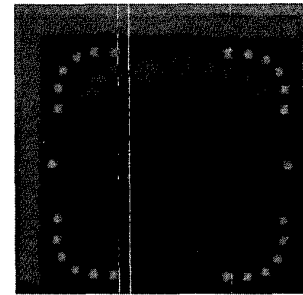


Figure 5: The MEMS wafer of the two-piece rocket included a 1mm diameter nozzle (at center). Across the nozzle, a nitride membrane suspended a polysilicon resistance igniter. Thermopiles suspended over thermal isolation holes surround the nozzle.

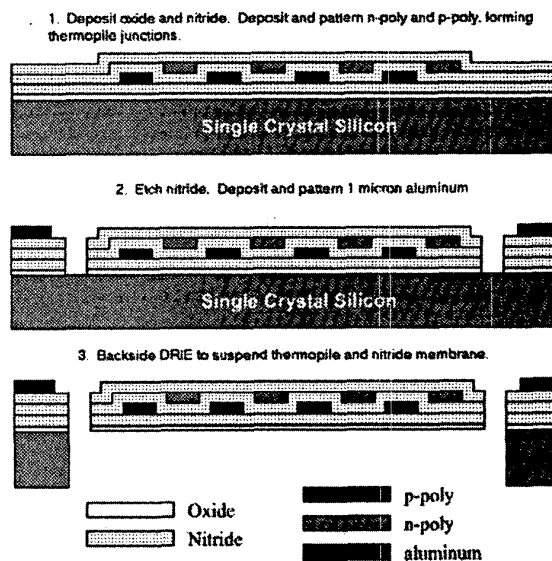


Figure 6: This is the summarized process flow used to fabricate the MEMS wafer for the two piece rocket. The etch that defined the nozzle also suspended the thermopiles.

diameter, and across that opening a polysilicon heater was suspended on a nitride membrane. Around the nozzle an array of twelve thermopiles were constructed. The MEMS wafer was fabricated by the process flow shown in Figure 6. The combustion chamber was filled with propellant by forcing it in with a spatula. After the fuel was cured, the cylinder was glued to the MEMS die with high temperature epoxy.

TESTING AND ANALYSIS

Testing began with the confirmation that the polysilicon igniter could in fact ignite the propellant. This test was successful, although it was discovered that the propellant needed to be in direct contact with the igniter to achieve ignition. Figure 7 shows a rocket during combustion. Each rocket was tested on a thrust apparatus comprised of a pendulum and a load cell. Passing current through the polysilicon heater ignited the fuel. Thrust was plotted vs. elapsed time. A typical thrust plot can be seen as Figure 8. The peak thrust obtained was 4mN, followed by a steady value of about 1.75mN was measured for the remainder of the combustion. By measuring the total length of the fuel chamber and the total duration of the combustion, an average reaction velocity was calculated to be about 1.7mm/sec. The corresponding I_{sp} for the figure was 14sec, or about 5.5% of the theoretical value for that fuel.



Figure 7: This is a photo of a ceramic combustion chamber during combustion.

The thrusts obtained were lower than expected, and were lower than the weight of the rocket, making flight on Earth impossible. If the continuity equation is applied at the burning surface and the outlet, and every cross-section downstream, we have:

$$\rho_1 v_1 A_1 = \rho_2 v_2 A_2 = \text{constant} \quad (3)$$

The mass flux into the control volume is the product of the solid fuel density (ρ_1), the cross sectional area of the combustion chamber (A_1), and the average burning velocity (v_1). The cross sectional area at the outlet is known (A_2) and the density (ρ_2) can be estimated by estimating the temperature and pressure. From equation (3), the outlet velocity of the combustion products was about 80 m/s or about one order of magnitude lower than the speed of sound at the estimated temperature of 1000K. This result indicated that the nozzle area could be reduced to accelerate the flow and increase thrust. Care must be taken, however not to make the throat too narrow, because viscous boundary

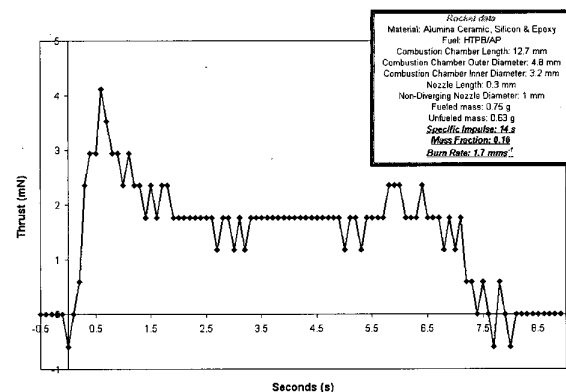


Figure 8: This is a typical thrust plot for a microrocket. The thrust of 1.75mN is less than the initial weight of the rocket (9.5mN). By increasing the thrust and decreasing the mass, light demonstrations are expected.

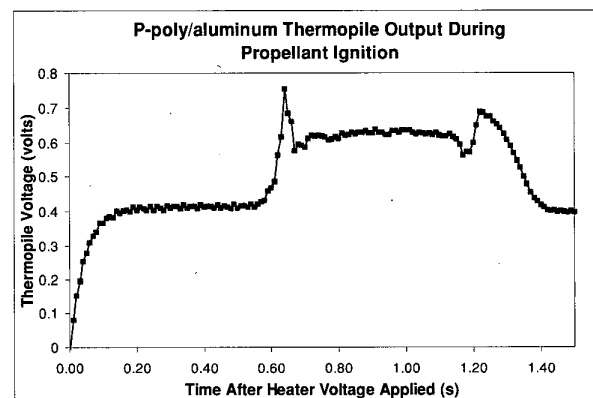


Figure 9: Thermopile voltage output during combustion. Ignition occurs at roughly 0.5s, and extinction occurs at 1.2s.

effects will dominate. Bayt et al reports supersonic flow in a diverging nozzle with a 20 μ m throat [14], confirming that narrower should be better.

The testing of the thermopiles was done separately from the thrust measurements. A resistor was placed across one of the twelve thermopiles, and the voltage across that resistor was measured during the combustion event. Typically 10-20microWatts were measured during these tests. See Figure 9.

THIRD-GENERATION DESIGN

Having established that combustion can sustain itself in a millimeter-scale rocket, a third generation of rocket was designed. The goals were to improve I_{sp} to 100sec and return to all-silicon fabrication. The design illustrated in Figures 11 was developed to achieve these goals. The stack of DRIE-fabricated chips offers a decreased surface area to volume ratio. Thermal isolation holes were included around the perimeter of each chip to

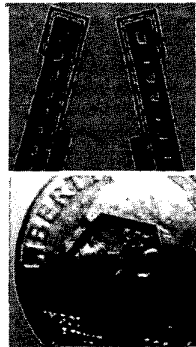
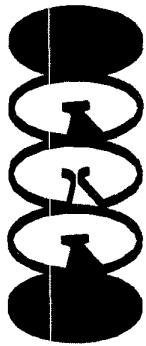


Figure 11: The all-silicon microrocket is a stack of components, as shown in the schematic drawing at left. The components were fabricated by DRIE. The individual component in the two images on the right represents the center layer, with the diverging nozzle. The close-up detail shows the silicon resistance igniter. The total outside diameter of each

further combat heat losses. A hexagonal shape was chosen in order to improve packing density on a 100mm wafer. Several components need to be stacked and bonded to enclose the fuel tank and make a complete rocket. The inside diameter of the hexagon was 8mm, and the thickness depends on the number of layers in the stack and the thickness of the wafers. Epoxy was used

to glue the layers together, although fusion bonding will be implemented in the future. While the total mass of fuel contained in this device is similar to the previous generation rocket, the total mass of the entire rocket was reduced by a factor of 3.

Throat widths of 300, 200, and 100 microns were included in the layout to test the trade-off between flow acceleration and viscous losses. While the corresponding throat areas are an order of magnitude smaller than the previous rocket, they are by no means beyond the lower limit.

Preliminary flight-testing has begun. The rocket described above has flown approximately 3 meters into the air, in an erratic 2sec flight (Figure 12). Examination of the combustion chamber showed that the epoxy had failed during combustion, allowing gaps to open between the layers. Improved assembly techniques, including fusion bonding, should help alleviate this problem.



Figure 12: Lift-off demonstration. Ignition was achieved (left), and the rocket took off (right). The flight lasted about 2s.

CONCLUSION

The feasibility of solid-propellant microrockets for near surface flight has been established. Measurable thrust and electric power have been obtained by a self-contained system. The third generation design has flown, and more rockets are being fabricated and tested. Future generations will contain sensing, control electronics, and actuated control surfaces.

REFERENCES

1. Yeh, R.; Pister, K.S.J. "Design of Low-Power Articulated Microrobots," Proc. International Conference on Robotics and Automation, Workshop on Mobile Micro-Robots, April 23-28, 2000, pp. 21-28.
2. Fearing, R.S. et al. "Wing Transmission for a Micromechanical Flying Insect," IEEE Int. Conf on Robotics and Automation, April 2000.
3. Bombardier Beetle website <http://www.owl.on.ca/owl/bbeetle.html>
4. J.M. Kahn, R.H. Katz, and K.S.J. Pister, "Emerging Challenges: Mobile Networking for Smart Dust", J. of Commun. And Networks, vol. 2, no. 3, September 2000.
5. Rossi, C. et al "A New Generation of MEMS Based Microthrusters for Microspacecraft Applications", Proc. MicroNanotechnology for Space Applications, Vol. 1, April 1999.
6. Borman, G.L., Ragland, K.W. *Combustion Engineering*. McGraw Hill. 1998.
7. <http://data.energizer.com/>
8. Mehra, A., Ayon, A., Waitz, I.A., Schmidt, M.A. "Microfabrication of High-Temperature Silicon Devices Using Wafer Bonding and Deep Reactive Ion Etching", IEEE Journal of MEMS, Vol. 8, No. 2, June 1999.
9. Seriburi, P., Kercher, D., Allen, M.G., 'An Experimental Study in Microfabricated Nickel-Iron Spark Plugs', Transducers '99.
10. Kelvin Fu, et al., "Preliminary Report on MEMS Rotary Internal Combustion Engine", 99F-023, Western States Section of the Combustion Institute, Fall Meeting, Irvine, CA, Oct. 25, 1999.
11. Munson, B.R., Young, D.F., Okiishi, T.H., "Fundamentals of Fluid Mechanics", pp. 591-611. Wiley & Sons. New York. 1998.
12. Lewis, D., Janson, S. Cohen, R., Antonsson, E. "Digital MicroPropulsion", Sensors and Actuators A: Physical, 2000, 80(2), pp. 143-154.
13. Olgun, Z. et al. "An Integrated Thermopile Structure with High Responsivity Using any Standard CMOS Process," A. Intl. Conference on Solid State Sensor and Actuators (Transducers '97), pp1263-1266, June 1997.
14. Bayt, R.L., Breuer, K.S., Ayon, A.A., "DRIE-Fabricated Nozzles for Generating Supersonic Flows in Micropropulsion Systems," Proceedings of the Solid-State Sensor and Actuator Workshop. Hilton Head, SC. June 1998.